⌘ *Author's Choice*

THE JOURNAL OF BIOLOGICAL CHEMISTRY VOL. 286, NO. 14, pp. 12308–12316, April 8, 2011

Lobe-specific Functions of Ca^{2+}·Calmodulin in αCa^{2+}·Calmodulin-dependent Protein Kinase II Activation*[S]

Received for publication, June 23, 2010, and in revised form, February 6, 2011 Published, JBC Papers in Press, February 7, 2011, DOI 10.1074/jbc.M110.157057

Abdirahman M. Jama[‡1], Jonathan Gabriel[‡1], Ahmed J. Al-Nagar[‡1], Stephen Martin[§], Sana Z. Baig[‡], Homan Soleymani[‡], Zawahir Chowdhury[‡], Philip Beesley[¶], and Katalin Török[‡2]

From the [‡]Division of Basic Medical Sciences, St. George's, University of London, Cranmer Terrace, London SW17 0RE, the [§]National Institute for Medical Research, The Ridgeway, Mill Hill, London NW7 1AA, and the [¶]School of Biological Sciences, Royal Holloway, University of London, Egham Hill, Egham TW20 0EX, United Kingdom

***N*-Methyl-D-aspartic acid receptor-dependent long term potentiation (LTP), a model of memory formation, requires Ca^{2+}·calmodulin-dependent protein kinase II (αCaMKII) activity and Thr^{286} autophosphorylation via both global and local Ca^{2+} signaling, but the mechanisms of signal transduction are not understood. We tested the hypothesis that the Ca^{2+}-binding activator protein calmodulin (CaM) is the primary decoder of Ca^{2+} signals, thereby determining the output, *e.g.* LTP. Thus, we investigated the function of CaM mutants, deficient in Ca^{2+} binding at sites 1 and 2 of the N-terminal lobe or sites 3 and 4 of the C-terminal CaM lobe, in the activation of αCaMKII. Occupancy of CaM Ca^{2+} binding sites 1, 3, and 4 is necessary and sufficient for full activation. Moreover, the N- and C-terminal CaM lobes have distinct functions. Ca^{2+} binding to N lobe Ca^{2+} binding site 1 increases the turnover rate of the enzyme 5-fold, whereas the C lobe plays a dual role; it is required for full activity, but in addition, via Ca^{2+} binding site 3, it stabilizes ATP binding to αCaMKII 4-fold. Thr^{286} autophosphorylation is also dependent on Ca^{2+} binding sites on both the N and the C lobes of CaM. As the CaM C lobe sites are populated by low amplitude/low frequency (global) Ca^{2+} signals, but occupancy of N lobe site 1 and thus activation of αCaMKII requires high amplitude/high frequency (local) Ca^{2+} signals, lobe-specific sensing of Ca^{2+}-signaling patterns by CaM is proposed to explain the requirement for both global and local Ca^{2+} signaling in the induction of LTP via αCaMKII.**

αCa^{2+}·calmodulin-dependent protein kinase II (αCaMKII)[3] (1) function is essential for memory formation, as demonstrated by studies of spatial learning (2) and of the electrophysiologically testable memory model, *N*-methyl-D-aspartic acid receptor (NMDAR)-dependent long term potentiation (LTP) (3, 4). A fundamental unexplained feature of the induction of LTP and memory formation is how global Ca^{2+} elevation is necessary but insufficient, while requiring additional local, high frequency NMDAR-mediated Ca^{2+} signals (5–8). αCaMKII is activated by Ca^{2+} stimulation in a frequency-dependent manner (9), and here we propose that Ca^{2+} signal transduction is determined by the activation mechanism of αCaMKII by Ca^{2+}·CaM.

αCaMKII is an abundant, neuronally expressed, broad specificity protein kinase that is especially enriched in the hippocampus, an area specialized in memory function. αCaMKII forms dodecamers (10), and its physiologically functional form is generated by autophosphorylation at residue Thr^{286} in the presence of ATP,[4] calmodulin (CaM), and elevated Ca^{2+} (11). αCaMKII thus differs from other Ca^{2+}·CaM-dependent protein kinases (CaMKs), *e.g.* CaMKI and CaMKIV, which are monomeric and for full activation require phosphorylation in the activation loop by an exogenous kinase, in addition to the Ca^{2+}·CaM binding-induced release of their autoinhibitory domain (12, 13). Activation is manifested in a switch-like increase in V_{max} as autoinhibited CaMKs have no detectable Ca^{2+}·CaM-independent basal activity. Later on, we will term this V type regulation. When the K_m values for ATP or protein substrates are affected, that will be termed K type regulation.

αCaMKII has two successive active states. The first active state is formed by the binding of Ca^{2+}·CaM and ATP. This complex is ready to phosphorylate protein or peptide substrates. Importantly, αCaMKII is a substrate for itself, and the αCaMKII active complex is converted to its second active state, Ca^{2+}·CaM·phospho-Thr^{286}-αCaMKII, by rapid autophosphorylation. This latter process is essential for NMDAR-dependent LTP and spatial learning (2, 4), although the functionally relevant target of the phosphoenzyme has not been identified. The Ca^{2+}·CaM binding affinity for the phosphoenzyme is $>10^4$-fold increased, and Ca^{2+} binding to CaM in the phosphoenzyme complex is stabilized when compared with that with nonphospho-αCaMKII (14). As a consequence, Ca^{2+}·CaM-bound phospho-Thr^{286}-αCaMKII exists not only at activating (>500 nM) but also at resting (<100 nM) free Ca^{2+} concentrations (14). At free Ca^{2+} concentrations of <20 nM, when Ca^{2+} and hence CaM dissociate, activity is reduced to ≤5% of that of fully Ca^{2+}·CaM-stimulated phospho-Thr^{286}-αCaMKII (14). Thus, phospho-Thr^{286}-αCaMKII activity is fully Ca^{2+}·CaM-dependent. Furthermore, the activity of phospho-Thr^{286}-αCaMKII is transient in LTP and is time-limited by inhibitory $Thr^{305/306}$ autophosphorylation (8, 15).

* This work was supported by Wellcome Trust Project Grant 075931 (to K. T.).
[S] The on-line version of this article (available at http://www.jbc.org) contains supplemental Materials and Methods, Tables S1–S3, and Figs. S1–S3.
⌘ *Author's Choice*—Final version full access.
[1] These authors contributed equally to this work.
[2] To whom correspondence should be addressed. Tel.: 44-2087255832; Fax: 44-2087253581; k.torok@sgul.ac.uk.
[3] The abbreviations used are: CaM, calmodulin; CaMK, Ca^{2+}·CaM-dependent protein kinase; CaMKII, Ca^{2+}·CaM-dependent protein kinase II; LTP, long term potentiation; NMDAR, *N*-methyl-D-aspartic acid receptor.
[4] ATP is used to indicate Mg^{2+}·ATP.

CaM, the Ca^{2+} binding activator of αCaMKII, is highly concentrated in neurons. CaM binds Ca^{2+} at four sites that are formed by EF-hand motifs, two at each of its N- and C-terminal lobes. Of these two lobes, the Ca^{2+} binding sites in the C-terminal lobe have inherently higher affinity for Ca^{2+} than those of the N-terminal lobe (16). Typically, both CaM lobes are involved in the activation of a wide range of CaM target enzymes, and the number of participating Ca^{2+} ions is thought to vary between 3 and 4 (17). To dissect the functions of the Ca^{2+} binding sites of CaM in αCaMKII activation, we have employed CaM mutants in which individual or multiple Ca^{2+} binding sites have been disabled. The mutants are termed CaM1, CaM2 (N lobe mutants), CaM3 and CaM4 (C lobe mutants), CaM12 and CaM34 (whole lobe mutants), and CaM1234 (the all-site mutant), indicating the position of the mutated EF-hand in the amino acid sequence (18).

The regulation of αCaMKII by CaM is complex. Binding and kinetic studies of Ca^{2+}·CaM and αCaMKII provided evidence for a dynamic process with a series of structural transitions in Ca^{2+}·CaM·αCaMKII during Ca^{2+}·CaM and ATP or ADP binding to the enzyme, in which process Ca^{2+}·CaM binding to αCaMKII is stabilized (19, 22). Ca^{2+}·CaM binding to αCaMKII is thought to be initiated by one of the CaM lobes, and evidence for such a role by either the N CaM lobe (20) or the C CaM lobe (21) has been presented. The initial Ca^{2+}·CaM-bound αCaMKII complex then undergoes a conformational change to and exists in equilibrium with a form in which CaM wraps around the CaM binding domain with both of its lobes bound (19). However, it is not clear how the signaling complexes formed by the interaction of Ca^{2+}, CaM, αCaMKII, and ATP transduce neuronal Ca^{2+}-signaling patterns that result in memory formation. Here we explored the hypothesis that at the molecular level, NMDAR-dependent LTP and memory formation are explained by lobe-specific differential sensing of global and local Ca^{2+} signals by CaM in the activation of αCaMKII.

MATERIALS AND METHODS

Proteins—αCaMKII was overexpressed in baculovirus-transfected Sf9 insect cells and purified by CaM-Sepharose and Mono Q FPLC. Wild type human liver recombinant calmodulin and its point mutants CaM1, CaM2, CaM3, CaM4, CaM12, CaM34, and CaM1234 were obtained by replacing their respective cDNAs from *Xenopus* vectors (kindly provided by J. P. Adelman) into *Escherichia coli* expression vectors (kindly performed by Dr. Nael Nadif Kasri, Catholic University of Leuven, Belgium). CaM mutants were generated by mutation of the first coordinating Asp of the Ca^{2+} binding EF-hand motifs to Ala. Mouse monoclonal anti-αCaMKII and anti-phospho-Thr^{286} antibodies were purchased from Chemicon.

Protein and Peptide Concentration Measurements—Protein concentrations were determined spectrophotometrically using molar extinction coefficients (ϵ_o) calculated from the amino acid composition: αCaMKII (subunits), $\epsilon_o = 64{,}805\ \text{M}^{-1}\ \text{cm}^{-1}$ (280 nm); CaM and CaM mutants, $\epsilon_o = 3{,}300\ \text{M}^{-1}\ \text{cm}^{-1}$ (278 nm) (19). Syntide 2 (23), purchased from Sigma-Aldrich, and the $\alpha\text{CaMKII}_{294-309}$ peptide (HPLC-purified to >95%) were measured by weight.

Steady-state Assay of αCaMKII Enzyme Activity—A continuous enzyme-linked spectrofluorometric assay was used to determine ADP production by monitoring the decrease in NADH fluorescence resulting from its oxidation to NAD^+ (19, 24). The assay was carried out at 21 °C in 50 mM K^+-PIPES, pH 7.0, 100 mM KCl, 2 mM $MgCl_2$. Typically, 5 mM DTT, 4.5 units of lactate dehydrogenase, 2 units of PK, 2 mM P-enolpyruvate, 22 μM NADH were added. Saturating concentrations were 2.5 μM free Ca^{2+}, 6 μM wild type or mutant CaM, 1 mM ATP, and 50 μM syntide 2. CaM34 was used at 60 μM in the presence of 220 μM Ca^{2+}. Ca^{2+}, CaM, syntide 2, and ATP concentrations were varied as specified in the appropriate figure legends. Baseline reading was obtained with all but αCaMKII in the assay mix, and 0.05 μM αCaMKII was added to observe enzyme activity in a 60-μl total volume. The fluorescence assays were carried out using an SLM spectrofluorometer and SLM 8100 software. Fluorescence excitation was set to 340 nm (bandpass of 2 nm), and emission was detected at 460 nm (bandpass 32 nm).

Thr^{286} Autophosphorylation of αCaMKII—Thr^{286} autophosphorylation time courses were measured by manual mixing. 1 μM αCaMKII, 6 μM CaM or CaM mutant (with the exception of CaM34, which was used at 60 μM in the presence of 220 μM Ca^{2+}), and 1 mM ATP were incubated in 50 mM K^+-PIPES, pH 7.0, 100 mM KCl, 2 mM $MgCl_2$, 5 mM DTT, and 0.05 mM $CaCl_2$ at 21 °C for various times from 0 to 1,800 s with 15 s as the shortest time point. The reaction was terminated using 4× SDS sample buffer at predefined time points. SDS-PAGE was carried out using 4–12% precast gels (Invitrogen). Thr^{286} autophosphorylation was visualized by Western blotting using a phospho-Thr^{286}-αCaMKII-specific monoclonal antibody and fluorescent secondary antibody (IRDye 800CW goat anti-mouse IgG). Imaging of Western blots on PVDF Immobilon transfer membranes (Millipore) was carried out using the Odyssey infrared imaging system (LI-COR Biotechnologies). Images were analyzed using ImageJ software (National Institutes of Health) as follows. The average density reading for each band on the Western blot and a reading for time 0 were taken. For time 0, the reaction was terminated prior to the addition of ATP. The following formula was used to calculate relative density on an inverted scale: $(D_{\max} - D_t)/(D_{\max} - D_B)$, where $D_{\max}$ is the average density of the darkest band, D_t is the average density at a particular time point, and D_B is the average density at time 0. The scale was thus inverted by subtracting each value from the highest density value. Relative density was calculated with reference to the highest density, and the data were fitted with exponential functions using GraFit software program, version 4.0.

Free Ca^{2+} Concentrations—Free Ca^{2+} concentrations were calculated using a K_d value of 4.35×10^{-7} M determined in similar buffer conditions, ionic strength, and pH to our assay buffer, which was composed of 50 mM K^+-PIPES pH 7.0, 100 mM KCl, 2 mM $MgCl_2$, 5 mM DTT, and appropriate Ca^{2+}/EGTA mixtures at 21 °C (25). To verify the calculated [Ca^{2+}] concentrations, the fluorescent Ca^{2+} indicator fluo3 was titrated in the assay solutions containing different Ca^{2+}/EGTA mixtures. The best fit to the titration curve gave a K_d value of 433 ± 55 nM for fluo3 in good agreement with the previously determined K_d value of 390 nM, thus verifying our calculated

$[Ca^{2+}]$ values (14). The effect of ATP was estimated to be negligible.

Software—A Fortran program solving the quadratic equation $[Ca^{2+}] = \{b \pm \cdot(b^2 - 4\times [Ca^{2+}]_o \times [EGTA]_o)\}/2$ where $b = K_d + [Ca^{2+}]_o + [EGTA]_o$ was used to calculate free Ca^{2+} concentration ($[Ca^{2+}]$) from total Ca^{2+} ($[Ca^{2+}]_o$), total EGTA ($[EGTA]_o$), and the K_d. Steady-state activity and autophosphorylation kinetic data were fitted to appropriate equations using GraFit version 4.0. Stopped-flow kinetic data were fitted using the KinetAsyst software (TgK Scientific). Enzyme kinetic data were simulated using Mathcad 2001i Professional. Analysis of variance with post hoc Dunnett's multiple comparison test was carried out using GraphPad Prism 5.

Statistical Analysis of the Data—Typically, three independent sets of experiments were carried out; the data were averaged and fitted to the Michaelis-Menten or the Hill equation. The error reported is the standard deviation (S.D.). A one-way analysis of variance was carried out to compare the K_m and V_{max} values across the mutants for each substrate and activator and for comparing the rates of Thr^{286} autophosphorylation stimulated by mutant CaMs with that of wild type CaM. Dunnett's multiple comparison test was performed as post hoc analysis for pairwise comparison of each mutant with the wild type data. Normality of distribution was tested by plotting a histogram of residuals and accepted by visual inspection of a bell-shaped distribution.

RESULTS

Characterization of EF-Hand CaM Mutants—The role of each Ca^{2+} binding site of CaM in the activation mechanism of αCaMKII was investigated to understand how signaling by Ca^{2+} influx is decoded by CaM in neurons. Firstly, the effect of mutating each EF-hand on CaM structure and function was characterized by comparing wild type and mutant Ca^{2+}·CaM secondary structure content and equilibrium and kinetic dissociation constants.

Far-UV CD spectroscopy, measured as described in supplemental Materials and Methods, demonstrated that there was no significant difference in helical structure content between wild type and mutant CaM in the presence of 0.2 mM EGTA (supplemental Fig. S1). Ca^{2+} binding by wild type CaM under conditions of 1 mM $CaCl_2$ caused a 1.24-fold increase in molar CD extinction coefficient at 222 nm ($\Delta\epsilon_{222}$, supplemental Table S1). The increases in $\Delta\epsilon_{222}$ induced by Ca^{2+} binding were smaller in the single mutant (1.4–1.9-fold) and further reduced in the double mutant (~1.1-fold) CaM proteins. The all-sites mutant CaM1234 far-UV CD spectrum was not altered by the presence of Ca^{2+} (data not shown). The effect of the mutations was thus approximately proportional to the number of mutated sites.

The stoichiometric Ca^{2+} dissociation constants of wild type and mutant CaMs, measured as described in supplemental Materials and Methods, were assigned to the N and C lobe, as established previously (26, 27). The overall dissociation constant for the N lobe was essentially unaffected in the C lobe mutants CaM3, CaM4, and CaM34, relative to wild type CaM (17 μM) (supplemental Fig. S2). Similarly, the overall dissociation constant for the C lobe in the N lobe mutants CaM1, CaM2, and CaM12 remained similar to wild type (1.8 μM). However, the N lobe dissociation constant was increased in the single N lobe mutants CaM1 (240 μM) and CaM2 (98 μM), in comparison with wild type, reflecting the lack of the second N lobe Ca^{2+} binding site. Similarly, the C lobe dissociation constant was increased in the single C lobe mutants CaM3 (30 μM) and CaM4 (12 μM) relative to wild type, due to the lack of the other C lobe Ca^{2+} binding site (supplemental Table S2).

Ca^{2+} dissociation kinetics of the Ca^{2+}-bound wild type and mutant CaM complexes, measured as described in supplemental Materials and Methods, were studied to determine the effect of mutation on the Ca^{2+} binding dynamics. The fluorescence increase of the Ca^{2+} chelator quin 2 upon trapping the dissociated Ca^{2+} was measured using stopped-flow spectroscopy. The complexes of Ca^{2+} bound to wild type and mutant CaMs with and without the $\alpha CaMKII_{294-309}$ target peptide were compared. In the absence of the peptide, the dissociation rate constant (k_{off}) of the C lobe site was essentially unchanged in the N lobe mutants CaM1, CaM2, and CaM12 with respect to wild type CaM (11.4 s^{-1}). The k_{off} of one of the N lobe sites was reduced to ~250 s^{-1} in the C lobe mutants CaM3, CaM4, and CaM34 when compared with wild type, for which the N lobe k_{off} was too fast to be measured and was estimated to be ~1,000 s^{-1} (28). Furthermore, Ca^{2+} dissociation rate constants of $\alpha CaMKII_{294-309}$ peptide complexes with wild type CaM and its mutants were reduced when compared with the corresponding peptide-free Ca^{2+} complexes, consistent with Ca^{2+}-dependent peptide binding (supplemental Table S3).

Thus, overall, the effect of each mutation in structural terms was localized to the respective, mutated EF-hand of CaM. Mutation of the N lobe sites had no significant effect on the Ca^{2+} binding properties of the C lobe sites (24). Mutation of site 3 or 4 revealed that the C lobe Ca^{2+} binding sites interact with one another and also affect the Ca^{2+} affinity of the N lobe.

Activation of αCaMKII by Single and Double EF-Hand Mutated CaMs—Substrate phosphorylation by αCaMKII activated by mutant CaM in comparison with wild type was studied using the steady-state NADH-coupled continuous fluorescence assay we had previously developed for the measurement of smooth muscle myosin light chain kinase activity (14, 15, 19, 22, 24). The steady-state kinetic parameters of αCaMKII activity were determined for each variable by keeping all other unvaried ligands at saturating concentrations, unless otherwise specified. This allowed derivation of the Michaelis-Menten constant and maximum velocity values for each variable (Table 1).

Syntide 2 Phosphorylation—Analysis of syntide 2 concentration dependences of steady-state αCaMKII activity fitted to the Michaelis-Menten equation showed that mutations of the Ca^{2+} binding sites of CaM did not affect the K_m value for syntide 2 given as 12.4 μM for wild type CaM (Fig. 1, Table 1). However, closer examination of Fig. 1, *B* and *C*, seemed to indicate that syntide 2 phosphorylation stimulated by C lobe CaM mutants may have been sigmoidal rather than hyperbolic. Thus, CaM3, CaM4, and CaM34 dependences were fitted to the Hill equation with the following results. The K_m and Hill coefficient (n) values were 7.56 ± 1.22 μM and 2.13 ± 0.69 for CaM3, 15.63 ± 3.17 μM and 1.74 ± 0.51 for CaM4, and 12.00 ± 2.32 μM and

TABLE 1

Kinetic parameters of steady-state αCaMKII activity stimulated by wild type and mutant CaMs

Each value represents the mean of three sets of measurements. The V_{max} values represent the mean of values obtained in the different substrate dependencies, and the error given is S.D.

	K_m of syntide 2	K_{act1} of Ca^{2+}	Hill coefficient of Ca^{2+}	K_{act2} of $Ca^{2+}{}_n$·CaM	K_{m4} of ATP	V_{max} (μmol of ADP)
	μM	μM	*n*	μM	μM	min^{-1} mg^{-1}
CaM	12.4 ± 2.9	0.50 ± 0.04	4.4 ± 1.3	< 0.05 ± 0.02[a]	46 ± 13	5.1 ± 1.2
CaM1	14.8 ± 5.5	1.56 ± 0.21	1.6 ± 0.3	2.9 ± 0.8	50 ± 17	1.8 ± 0.6[b]
CaM2	22.0 ± 6.4	0.75 ± 0.07	4.0 ± 1.8	0.7 ± 0.1	60 ± 16	3.8 ± 0.5
CaM3	7.8 ± 2.7	1.03 ± 0.04	4.3 ± 0.7	1.2 ± 0.9	188 ± 37[b]	2.1 ± 0.3[b]
CaM4	22.0 ± 7.5	0.65 ± 0.08	2.4 ± 0.7	1.4 ± 0.6	80 ± 42	2.3 ± 0. 5[b]
CaM12	23.7 ± 8.2	0.50 ± 0.09	1.8 ± 0.5	< 0.05 ± 0.02[a]	59 ± 11	1.9 ± 0.7[b]
CaM34	37.5 ± 25	64 ± 4[b]	3.2 ± 0.6	87 ± 25[b]	119 ± 22[b]	2.2 ± 0.7[b]

[a] Determined in the presence of 100 nM enzyme.

[b] Indicates significant difference from the value of the given parameter for wild type CaM. Significance was determined as described under "Materials and Methods."

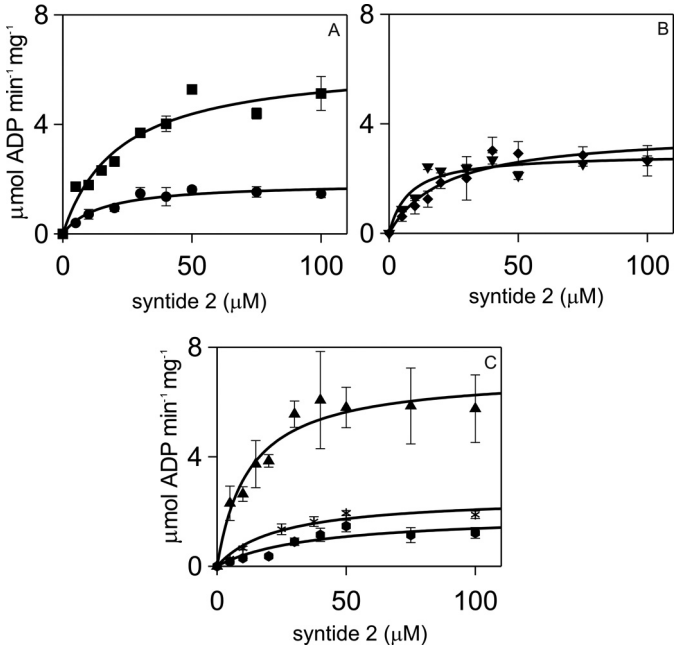

FIGURE 1. **Kinetic parameters of αCaMKII activity stimulated by wild type and mutant CaMs, with respect to syntide 2 substrate.** Steady-state activity measurements were carried out as described under "Materials and Methods." CaM or CaM mutants were used at 6 μM, and the free Ca^{2+} concentration was 2.5 μM, except for CaM34, which was present at 60 μM concentration and for which [Ca^{2+}] of 100 μM was used. αCaMKII concentration was 50 nM, and ATP concentration was 1 mM. The panels show CaM1 (●) and CaM2 (■) (*A*); CaM3 (▼) and CaM4 (◆) (*B*); and CaM12 (✳), CaM34 (●), and wild type CaM (▲) (*C*). The *error bars* represent the S.D. from three sets of data.

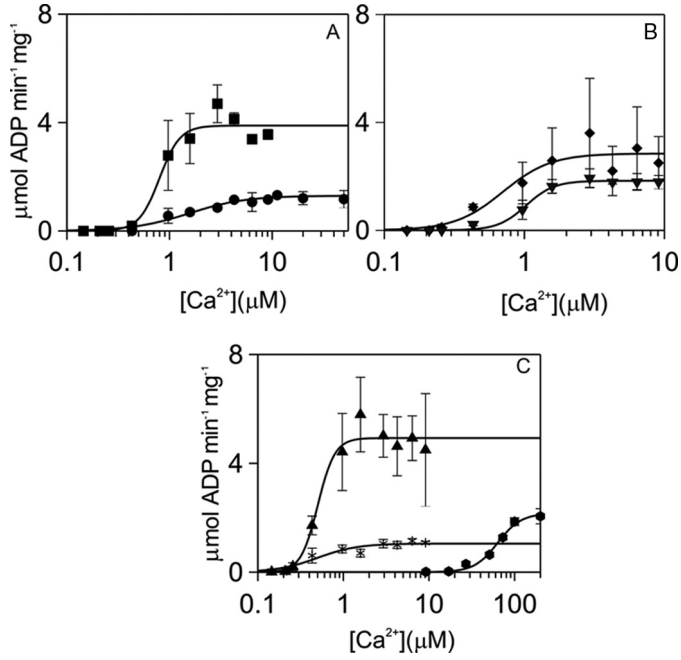

FIGURE 2. **Kinetic parameters of αCaMKII activity stimulated by wild type and mutant CaMs, with respect to [Ca^{2+}].** Steady-state activity measurements were carried out, and free Ca^{2+} concentrations were determined as described under "Materials and Methods." Syntide 2 concentration was 50 μM. CaM or mutants were used at 6 μM, except for CaM34, which was present at 60 μM. αCaMKII concentration was 50 nM, and ATP concentration was 1 mM. The panels show CaM1 (●) and CaM2 (■) (*A*); CaM3 (▼) and CaM4 (◆) (*B*); CaM12 (✳), CaM34 (●), and wild type CaM (▲) (*C*). The *error bars* represent the S.D. from three sets of data.

1.49 ± 0.43 for CaM34, respectively. The *n* values for CaM3 and CaM4 were close to 2, suggesting that Ca^{2+}·CaM C lobe interactions may affect peptide substrate binding to αCaMKII.

Ca^{2+} and Ca^{2+}·CaM Activation of αCaMKII—Ca^{2+} dependences of activation of syntide 2 phosphorylation by αCaMKII were compared for wild type CaM and CaM mutants (Fig. 2). The Ca^{2+} activation constant K_{act1} for wild type CaM was ~500 nM with a Hill coefficient (*n*) of 4.4 (Table 1), comparable with that measured for smooth muscle myosin light chain as substrate (14). Multiple comparison of the K_{act1} values showed no significant difference between wild type CaM and the mutants, with the exception of CaM34, for which the K_{act1} value was 64 μM (Table 1).

Ca^{2+}·CaM activation constant K_{act2} values were derived from CaM dependence experiments shown in supplemental Fig. S3. Although the K_{act2} for wild type CaM and CaM12 appeared lower than those for the other mutants, multiple comparison revealed no significant difference between the wild type and mutant CaMs apart from the K_{act2} for CaM34, which was significantly higher at 87 μM (Table 1).

ATP and Ca^{2+}·CaM in the Activation of αCaMKII—ATP binding stabilizes Ca^{2+}·CaM binding to αCaMKII by lowering the K_d for Ca^{2+}·CaM 10-fold (19, 22). This relationship was expected to be reciprocal with Ca^{2+}·CaM binding increasing ATP affinity for αCaMKII. Measurement of the dependence of αCaMKII activity on ATP concentration in the presence of the CaM mutants was expected to reveal whether the stabilizing effect of CaM was specifically localized to any of its Ca^{2+} binding site(s). The Michaelis-Menten constant K_{m4} for ATP of 46 μM measured in the presence of wild type CaM for syntide 2 phosphorylation was similar to that previously measured with smooth muscle myosin light chain as substrate (14). Remarkably, the K_m for ATP remained unchanged with the N lobe

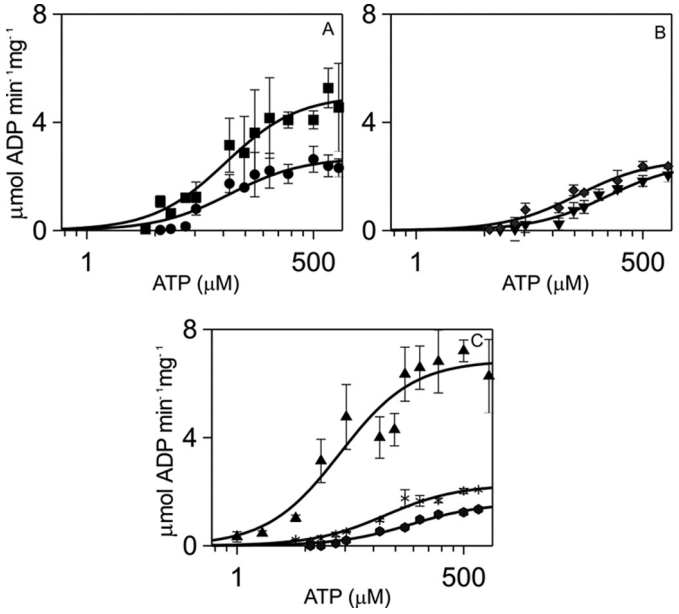

FIGURE 3. **Kinetic parameters of αCaMKII activity stimulated by wild type and mutant CaMs, with respect to [ATP].** Steady-state activity measurements were carried out as described under "Materials and Methods." Syntide 2 concentration was 50 μM, free [Ca^{2+}] concentration was 1.58 μM, and CaM or mutants were used at 6 μM, except for CaM34, which was present at 60 μM concentration and for which [Ca^{2+}] of 100 μM was used. αCaMKII concentration was 50 nM. The panels show CaM1 (●) and CaM2 (■) (*A*); CaM3 (▼) and CaM4 (◆) (*B*); CaM12 (✳), CaM34 (●), and wild type CaM (▲) (*C*). The *error bars* represent the S.D. from three sets of data.

mutants CaM1, CaM2, and CaM12 and C lobe mutant CaM4. In contrast, the K_m values for ATP were significantly increased with C lobe mutants CaM3 and CaM34, ~4- and 3-fold, respectively (Fig. 3, Table 1). Thus, the interaction that couples the ATP and Ca^{2+}·CaM binding sites resides in the CaM C lobe and is effected by site 3.

Turnover Rate—V_{max} values displayed by αCaMKII were measured for each CaM mutant to identify the role of each Ca^{2+} binding site and lobe in determining the αCaMKII turnover rate. The V_{max} value for wild type CaM was 5.1 μmol of ADP min^{-1} mg^{-1} enzyme. A significant difference ($p < 0.05$) was revealed in the V_{max} values for all but the CaM2 mutant when compared with wild type CaM (Figs. 1–3, Table 1). Mutation of EF-hands 1, 3, or 4 resulted in reducing V_{max} to 20–40% of that given by wild type CaM (Fig. 1*B*, Table 1). To check that saturating conditions were reached, CaM1 activity was measured at 10 μM in the presence of 50 μM Ca^{2+} and at 30 μM CaM1 in the presence of 100 μM Ca^{2+}. These conditions did not further increase V_{max} for CaM1, and any further increases resulted in reduced activity. The whole lobe mutants CaM12 and CaM34 showed similar reductions in activity (Fig. 1*C*, Table 1). For completeness, it needs to be noted that the all-sites mutant CaM1234 induced no measurable αCaMKII activity (data not shown).

In summary, the steady-state activity data showed that occupancy of Ca^{2+} binding sites 1, 3, and 4 of CaM was necessary and sufficient to stimulate full activity of αCaMKII; thus, neither the N nor the C lobe alone was sufficient to fully activate the enzyme. The C lobe of Ca^{2+}·CaM acted as a regulator of ATP affinity, via site 3, suggesting distinct roles for the N and C lobes of CaM.

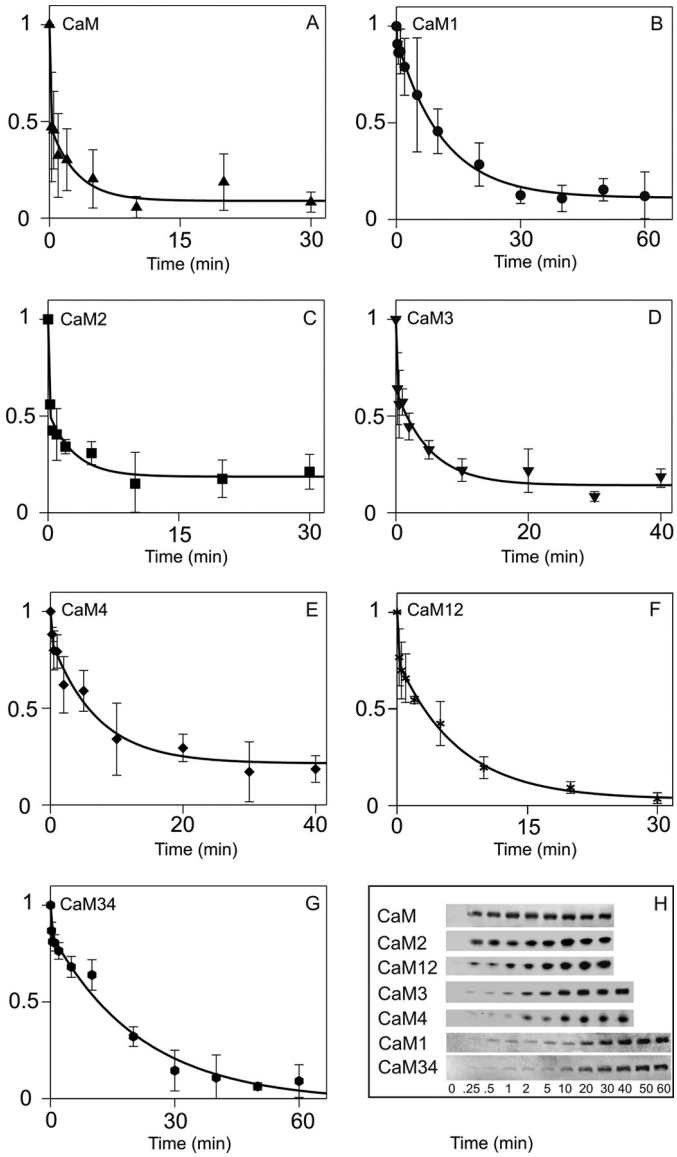

FIGURE 4. **Thr^{286} autophosphorylation time courses of αCaMKII activated by wild type and mutant CaMs.** *A–G*, Western blots (shown in *H*) for CaM (*A*), CaM1 (*B*), CaM2 (*C*), CaM3 (*D*), CaM4 (*E*), CaM12 (*F*), and CaM34 (*G*) were analyzed by densitometry as described under "Materials and Methods" and by fitting the inverted relative density to an exponential function. The deduced rate constants and relative amplitudes are shown in Table 2. *H*, Western blots of Thr^{286} autophosphorylation time courses were stimulated by wild type CaM, CaM1, CaM2, CaM3, CaM4, CaM12, and CaM34, as indicated. The *error bars* represent the S.D. from three sets of data.

Thr^{286} Autophosphorylation of αCaMKII Stimulated by Wild Type and Mutant CaMs—Our time courses of Thr^{286} autophosphorylation monitored by Western blotting showed biphasic kinetics with wild type CaM (Fig. 4, *A* and *H*). At 21 °C, the first phase, representing ~50% of the amplitude, proceeded at an estimated rate of 5 s^{-1}. The second phase of similar amplitude followed with a rate of 0.006 s^{-1} (Table 2). Thr^{286} autophosphorylation activated by CaM2 and CaM3 showed similar time courses to that with wild type CaM. In contrast, in the time course of Thr^{286} autophosphorylation activated by CaM1, CaM4, CaM12, and CaM34, the fast phase was much diminished, and rates of the second phase were significantly slower at 0.0014, 0.002, 0.0024, and 0.0008 s^{-1} ($p < 0.05$), respectively.

TABLE 2

Analysis of Thr^{286} autophosphorylation time courses stimulated by mutant CaMs

Time courses of Thr^{286} autophosphorylation were best fitted to a double exponential function. For each phase, the observed rate and relative amplitude are given. Each value represents the mean of three sets of measurements. The error given is S.D., except for the first phase, for which the observed rate is estimated from the start and endpoints.

	k_1	A_1	k_2	A_2
	s^{-1}		s^{-1}	
CaM	5 ± 0	0.6 ± 0.1	0.006 ± 0.002	0.4 ± 0.1
CaM1	5 ± 0	0.1 ± 0.03	0.0014 ± 0.0001[a]	0.9 ± 0.02
CaM2	5 ± 0	0.6 ± 0.1	0.006 ± 0.003	0.4 ± 0.1
CaM3	5 ± 0	0.4 ± 0.1	0.003 ± 0.001	0.6 ± 0.1
CaM4	3 ± 0	0.2 ± 0.11	0.002 ± 0.001[a]	0.8 ± 0.1
CaM12	5 ± 0	0.2 ± 0.1	0.0024 ± 0.0003[a]	0.8 ± 0.1
CaM34	5 ± 0	0.14 ± 0.06	0.0008 ± 0.0002[a]	0.86 ± 0.07

[a] Indicates significant difference from the rate of the second phase of Thr^{286} autophosphorylation obtained for wild type CaM. Significance was determined as described under "Materials and Methods."

In conclusion, Ca^{2+} binding to a site on each lobe, site 1 on the N lobe and site 4 on the C lobe, as well as the participation of both the N and the C CaM lobes are necessary for rapid Thr^{286} autophosphorylation.

DISCUSSION

CaM Mutants—In the present work, CD measurements were conducted at physiological ionic strength and in the presence of 1 or 2 mM Mg^{2+}. In these conditions, the effects of the mutations were limited to the mutated EF-hand(s) and were less severe than those previously reported for CaM12, CaM34, and CaM1234, which were measured at low ionic strength and in the absence of Mg^{2+} (30). Thus, the CaM mutants demonstrated structural integrity and therefore suitability for studying the function of individual Ca^{2+} binding sites of CaM in the activation of αCaMKII.

Although in wild type CaM dissociation from the N lobe Ca^{2+} binding sites is ~1,000 s^{-1} (27), a Ca^{2+} dissociation rate constant of ~250 s^{-1} was measured for single site mutants CaM3 and CaM4 and the double C lobe mutant CaM34 in which there were no functional C lobe Ca^{2+} binding sites (supplemental Table S3). In the CaM34 mutant, this rate constant indicated unmasking of negative cooperativity (30). However, in our single EF-hand mutants, similarly to previously described *Drosophila* CaM mutants in which Ca^{2+} binding function was disabled by mutation of the last glutamic acid residue of the EF-hands to alanine (28), similar rate constant values showed the loss of positive cooperativity between the C lobe Ca^{2+} sites by the mutation.

K_m values for syntide 2 were largely unaffected by mutation of the Ca^{2+} binding sites of CaM. Closer analysis, however, revealed possible cooperativity in syntide 2 phosphorylation stimulated by C lobe mutants CaM3 and CaM4. Previously, n values of 2.4 ± 0.3 and 2.3 ± 0.1 have been described for smooth muscle myosin light chain phosphorylation by αCaMKII and the T286A αCaMKII mutant (22). Further work is required to determine the underlying mechanisms.

K_{act2} values for wild type CaM and CaM12 were in the range of the enzyme concentration of 50–100 nM used in the assay, allowing the estimation of the K_{act2} of <50 nM. K_{act2} values for the other mutant CaMs were more than 10-fold higher, which allowed their accurate determination.

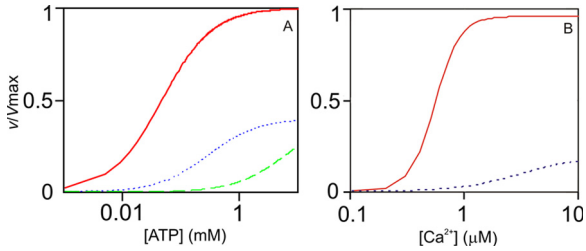

FIGURE 5. **Simulation of K and V type regulation of αCaMKII.** *A*, Equation 1 was used with K_{m4} and V_{max} values for wild type CaM (*solid line*) and CaM3 (dotted and *dashed line*) mutant (Table 1), with [ATP] at 1 mM. The previously determined value of 80 nM was used for K_{d3}, the dissociation constant for $Ca^{2+}{}_n$·CaM binding to αCaMKII·ATP (22). The *dotted line* represents data at 6 μM CaM3, and the *dashed line* represents data at 0.1 μM CaM3. K type switch is indicated by the substantial left shift of the activation curve by increasing the Ca^{2+}·CaM concentration and by occupancy of EF-hand 3 in the CaM C lobe. *B*, Equation 2 was used with parameters V_{max}, K_{act1}, n, and K_{m4} values for wild type CaM (*solid line*) and CaM1 mutant (*dotted line*), as shown in Table 1, with [ATP] at 1 mM. The V type activity switch is demonstrated by the large jump in activity by occupancy of the N lobe EF-hand 1. Equation 1, $v = k_{cat}[\alpha CaMKII]_o/(1 + K_{m4}/[ATP] + K_{d3}/[Ca^{2+}{}_n\cdot CaM] + K_{d3}K_{m4}/[ATP][Ca^{2+}{}_n\cdot CaM])$, where n is the measured Hill coefficient. Equation 2, $v = k_{cat}[\alpha CaMKII]_o/(1 + K_{m4}/[ATP] + K_{act1}{}^n/[Ca^{2+}]^n + K_{act1}{}^n K_{m4}/[Ca^{2+}]^n[ATP])$, where n is the measured Hill coefficient.

K Type Regulation of αCaMKII by the Ca^{2+}/CaM C Lobe with Respect to ATP—$Ca^{2+}{}_n$·CaM binding is stabilized by ATP binding to αCaMKII (19, 22, 31). Abolition of the CaM C lobe Ca^{2+} binding site 3 obliterated the interaction between the Ca^{2+}·CaM and ATP binding sites, showing that binding of the CaM C lobe, but not the N lobe, stabilizes ATP binding to αCaMKII. Considering $Ca^{2+}{}_n$·CaM and ATP as the activator and substrate in a rapid equilibrium steady-state scheme, simulated curves of activation by wild type CaM and CaM3 were in good agreement with the measured data. Thus, without the engagement of site 3, ATP affinity is much diminished, even with $Ca^{2+}{}_n$·CaM in excess, as used in the assay (Figs. 4, *A* and *C*, and 5*A*). Moreover, as the K_m for ATP (K_{m4}) is dependent on the concentration of $Ca^{2+}{}_n$·CaM, a further decrease in ATP affinity results in essentially no activity at limiting concentrations of $Ca^{2+}{}_3$·CaM3, even at 1 mM ATP concentration (Fig. 5*A*). As the CaM C lobe acts on the K_m for ATP, this is viewed as a K type switch. As shown in Fig. 5*A*, this primes but does not activate αCaMKII.

V Type Activation of αCaMKII by CaM N Lobe Ca^{2+} Binding Site 1—Comparing V_{max} values evoked by CaM mutants, lack of occupancy of Ca^{2+} binding sites 1, 3 and 4 was found to severely impair αCaMKII activity. The Ca^{2+} activation curves of wild type CaM and CaM1 were simulated by feeding the measured and estimated steady-state parameter values into Equation 2 (see legend for Fig. 5). As shown in Fig. 5*B*, the simulated curves are in good agreement with the measured data (Fig. 2, *A* and *C*). Although with wild type CaM, maximum turnover rate is achieved with a midpoint of 500 nM $[Ca^{2+}]$, the activity at this $[Ca^{2+}]$ concentration in the absence of EF-hand 1 Ca^{2+} occupancy is negligible. As occupancy of N lobe EF-hand 1 primarily affects the enzyme turnover rate, it is concluded that Ca^{2+} binding site 1 of the CaM N lobe acts as a V type activity switch in αCaMKII activation. Occupancy of C lobe Ca^{2+} binding sites 3 and 4 is also required for full activation, and thus, both lobes of CaM participate in the process.

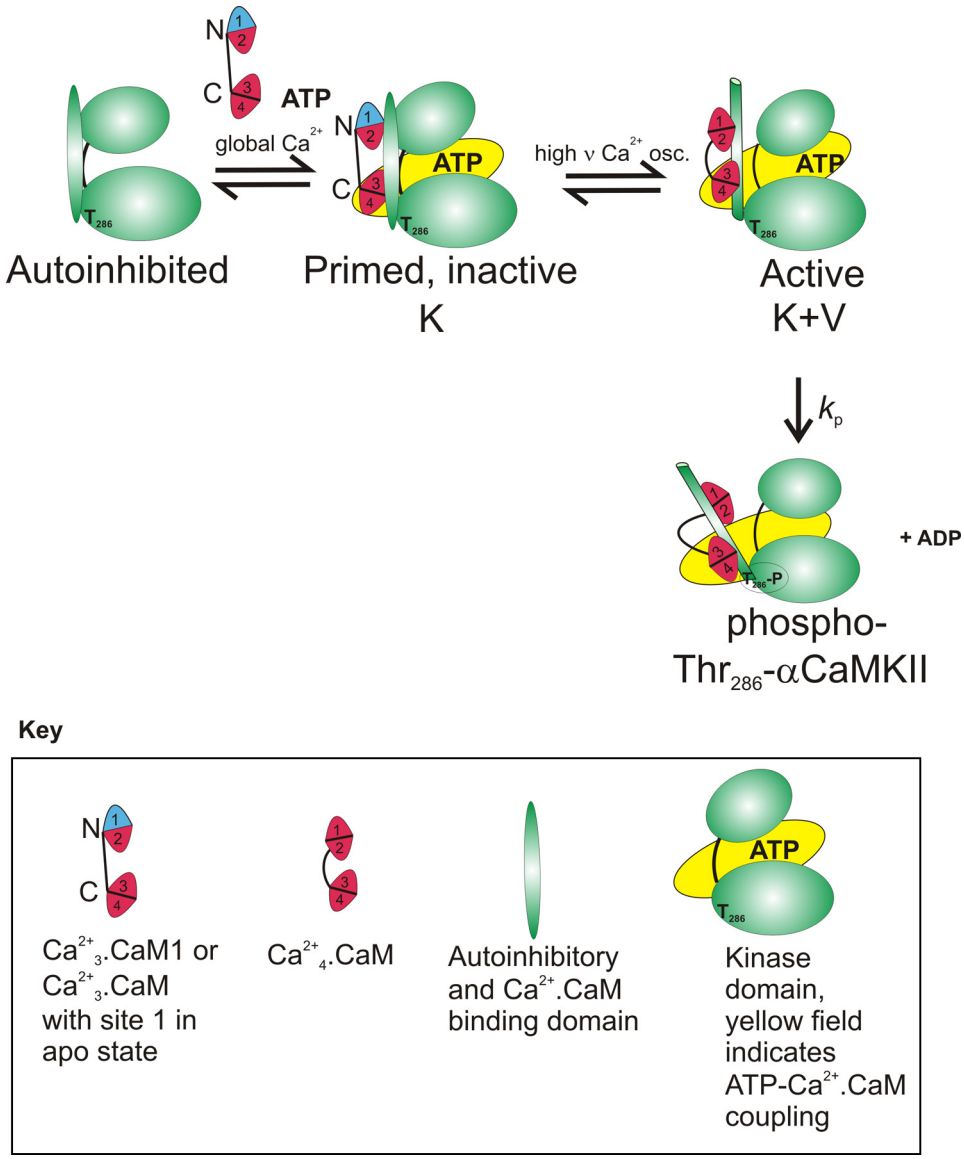

SCHEME 1. **Diagram to illustrate the function of the V type activity switch of K activation-primed αCaMKII by high frequency and amplitude Ca^{2+} signals via Ca^{2+} binding to N lobe site 1.**

Ca^{2+} Binding Sites 1, 3, and 4 of CaM Are Necessary and Sufficient for αCaMKII Activation—Interestingly, Ca^{2+} binding site 2 in the N lobe appeared unnecessary, and Ca^{2+} binding to site 2 was insufficient for activation. Site 2, however, may be significant in ensuring that the CaM N lobe is involved in binding to αCaMKII even when site 1 is not filled. The anomalous behavior of CaM12 may thus be explained by the absence of site 2, allowing single lobe CaM interaction with αCaMKII. This may not occur with wild type CaM, which is likely to preferentially engage in bilobal interactions. This is taken into account when formulating Scheme 1.

Thr^{286} Autophosphorylation of αCaMKII by the K-V Double Switch—Ca^{2+}·CaM-dependent autophosphorylation at Thr^{286} is of fundamental importance in the physiological functioning of αCaMKII (2). The rate constant for Thr^{286} autophosphorylation has not been precisely determined, but available evidence suggests it to be high. The highest estimate for the rate of Thr^{286} autophosphorylation at 21 °C is ~5 s^{-1}. This was based on the indirect measurement of Ca^{2+}·CaM trapping-induced partial activity by quenched flow (29). In our previous manual mixing experiments, monitoring Thr^{286} autophosphorylation by Western blotting for 2 min, wild type CaM-induced Thr^{286} autophosphorylation appeared complete within 15 s (14). When following the reaction for up to 60 min, however, a second slow phase has become apparent (Fig. 4, *A* and *H*, Table 2). Our data suggest that initial rapid Thr^{286} phosphorylation of ~50% of the subunits of the αCaMKII dodecamers is followed by slower phosphorylation of the other half. It will be important to determine the significance of the rapid initial Thr^{286} autophosphorylation and the precise temporal relationship between the phases of Thr^{286} autophosphorylation and inhibitory $Thr^{305/306}$ autophosphorylation (15).

In the absence of Ca^{2+} binding to sites 1 or 12, Thr^{286} autophosphorylation was too slow to be physiologically significant, demonstrating that V type activation of αCaMKII was required for its rapid activation. Significantly slower Thr^{286} autophos-

phorylation activated by CaM4 and CaM34 highlights the requirement for K type activation by the CaM C lobe for rapid Thr^{286} autophosphorylation of αCaMKII. These data suggest that both lobes of Ca^{2+}·CaM and the K-V double switch are required for rapid Thr^{286} autophosphorylation (Fig. 4, Table 2).

Single Lobe Association of CaM with Phospho-Thr^{286}-αCaMKII—Double mutants that have both Ca^{2+} sites mutated in one of the lobes of CaM allow testing lobe-specific CaM functions. However, as CaM is a bilobally functional protein, its single functional lobe mutants may not mimic the behavior of the native protein in every respect. In the absence of a functional N lobe, the CaM C lobe could partially substitute for the function of the N lobe and vice versa, similarly to how in some Ca^{2+}-dependent interactions, an unmutated Ca^{2+} binding lobe can substitute for the Ca^{2+} binding-deficient lobe in its interactions with gap junction protein connexin 32-derived CaM binding peptides (30).

However, there may be a role for wild type CaM Ca^{2+}-bound C lobe attachment in physiological conditions to phospho-Thr^{286}-αCaMKII, as follows. Ca^{2+} chelation causes biphasic dissociation of Ca^{2+} and CaM from their complex with phospho-Thr^{286}-αCaMKII. Partial dissociation occurs in the rapid first phase, but progress to full dissociation by the slower second phase requires [Ca^{2+}] concentrations <20 nM. At [Ca^{2+}] concentrations in the range of 20–500 nM, partially Ca^{2+}-bound CaM remains attached to phospho-Thr^{286}-αCaMKII (14). The point of attachment is likely to be the CaM C lobe so that a ($Ca^{2+}{}_2$·CaM_C)·phospho-Thr^{286}-αCaMKII·ATP complex would exist, anchoring CaM to the phospho-enzyme after intracellular Ca^{2+} has returned to resting levels. This complex could then be reactivated by subsequent Ca^{2+} elevations by CaM N lobe Ca^{2+} binding. The responses of this complex to Ca^{2+} signals are likely to be important in post-LTP synaptic plasticity. Reactivation may be limited to a window by timed auto-inactivation and $Thr^{305/306}$ autophosphorylation of phospho-Thr^{286}-αCaMKII (15).

Frequency Dependence of αCaMKII activation by Pulsatile Ca^{2+} Signals—In our steady-state experiments, the active complex was formed in the presence of saturating ligands. The presence of Ca^{2+} at a constant concentration can be viewed as persistently elevated, whereas in physiological systems, the temporal pattern of Ca^{2+} signals is decisive in the output. Due to the fast kinetics of Ca^{2+} binding and dissociation, the CaM N lobe would be the first to bind Ca^{2+} when stimulated by low frequency signals, but this Ca^{2+} would rapidly dissociate from the N lobe and associate with the higher affinity C lobe sites.

Scheme 1 shows the autoinhibited state of αCaMKII. However, the work presented here does not address the order of ATP and CaM binding to αCaMKII or the order in which the Ca^{2+}·CaM N and C lobes may bind. Thus, although the model shows that ATP and Ca^{2+}·CaM need to bind to αCaMKII to activate it, the order of binding is not discussed here.

Our data show that N lobe alone is insufficient either to activate or to affect ATP binding and that the Ca^{2+}·CaM C lobe is required for ATP coupling but is not sufficient for activation. We thus argue that CaM C lobe binding could be stabilized by ATP and that the "primed" state could be produced at relatively low Ca^{2+} concentrations as a result of a single spike or global Ca^{2+} rise; in contrast, activation by N lobe site occupancy requires high amplitude and/or frequency signals. Furthermore, our data for CaM12 and CaM34 indicate that single lobe interactions would substantially differ from bilobal ones. As at present there is no evidence to suggest that in physiological conditions, only one CaM lobe is available for αCaMKII activation, our conclusions and model are based on the single site mutants of CaM, which permit the involvement of both CaM lobes in αCaMKII activation.

A conceivable intermediate could be a C lobe-attached Ca^{2+}·CaM_C·αCaMKII·ATP complex. However, our data suggest that a likely intermediate is a $Ca^{2+}{}_3$·CaM·αCaMKII·ATP complex, in which CaM Ca^{2+} sites 2, 3, and 4 are filled. This intermediate corresponds to that formed by the CaM1 mutant. It lacks activity, but in it, both CaM lobes are engaged, and it is primed by K type activation via the CaM C lobe. Scheme 1 depicts how this intermediate is activated by the V type switch by high frequency Ca^{2+} signals able to populate site 1. Once activated, the enzyme undergoes rapid Thr^{286} autophosphorylation.

By requiring both a K and a V type switch and in that the two functions reside in separate Ca^{2+} binding lobes of CaM, αCaMKII represents a special case of Ca^{2+}·CaM target. Although lobe-specific functions of CaM are commonly seen in the regulation of ion channels (33), such distinction is shown for the first time here in the regulation of protein kinase function. CaM lobe-specific decoding of local and global Ca^{2+} signals is a novel principle in downstream signaling to kinases generating an altered state of the target by autophosphorylation. The K-V double switch sharpens the activation of αCaMKII likening it to a binary switch.

LTP Induction Explained by Lobe-specific Decoding of Ca^{2+} Signals by CaM in the Activation of αCaMKII—The mechanism outlined in Scheme 1 also explains why global Ca^{2+} signaling is not sufficient but local stimulation is required for NMDAR-dependent LTP induction (2, 7, 8). Global Ca^{2+} transients of low amplitude and frequency are sufficient to activate the K switch and thereby to prime but not activate αCaMKII. However, high amplitude and high frequency local Ca^{2+} stimulation is required for occupancy of CaM N lobe Ca^{2+} site 1, the V type activity switch. Once the αCaMKII active complex is formed, rapid Thr^{286} autophosphorylation and LTP induction follow. Thus, separate functions in activating αCaMKII coupled with differential Ca^{2+} sensing by the C and N lobes enable CaM to selectively decode global and local Ca^{2+} signals and explain the frequency dependence of αCaMKII activation and of LTP induction.

To sense local Ca^{2+} transients, CaM and αCaMKII need to be localized at the postsynaptic membrane in the vicinity of glutamate receptor channels, but the mechanisms ensuring this have not been clearly established (34–38). Thr^{286} autophosphorylation has been proposed to be the key to memory-forming interactions of αCaMKII as opposed to its self-association (39). However, the precise nature of such interactions has not been identified.

Using computationally designed mutations to stabilize the inactivated Ca^{2+} binding lobes in the "closed" apo-conformation, it has been suggested that CaM with two Ca^{2+} ions bound

to its C lobe not only binds αCaMKII with low μM affinity but also partially activates kinase activity. It was thus concluded that activation of αCaMKII by the CaM C lobe alone likely contributes to activation during small increases in Ca^{2+} in the dendritic spines (40). Our data with CaM12 suggest that in the absence of functional N lobe Ca^{2+} binding sites, the CaM C lobe appears sufficient for partial activation of αCaMKII. However, if at least one N lobe site is also functional, the activation mechanism appears to be different. Our previous work concluded that single lobe CaM association, likely the C lobe, may be of significance after activation, in association with phospho-Thr^{286}-αCaMKII (14). It requires further work to determine whether C lobe-only interactions are physiologically relevant. Cellular experiments will be required to determine the correlation between effects of the CaM mutants on αCaMKII activation *in vitro* and in intact cells. High levels of endogenous CaM make that a challenging project.

In summary, separate K type and V type regulation by the C and N CaM lobes in the activation of αCaMKII is demonstrated. ATP binding has been known to stabilize CaM binding to αCaMKII (19, 31), but lobe specificity by CaM in this interaction is a novel finding. The K switch makes αCaMKII an extremely efficient receptor of small amounts of locally released Ca^{2+}, and the K-V double switch ensures that activated αCaMKII undergoes rapid Thr^{286} autophosphorylation.

Acknowledgments—We thank Elizabeth R. Morris (University of Nottingham) for comments on the manuscript and for useful discussions. We thank M. Lacey (St George's, University of London) for help with Western blotting and imaging with the Odyssey system.

REFERENCES

1. Colbran, R. J., and Brown, A. M. (2004) *Curr. Opin. Neurobiol.* **14,** 318–327
2. Giese, K. P., Fedorov, N. B., Filipkowski, R. K., and Silva, A. J. (1998) *Science* **279,** 870–873
3. Bliss, T. V., and Lomo, T. (1973) *J. Physiol.* **232,** 331–356
4. Malenka, R. C., Kauer, J. A., Perkel, D. J., Mauk, M. D., Kelly, P. T., Nicoll, R. A., and Waxham, M. N. (1989) *Nature* **340,** 554–557
5. Topolnik, L., Chamberland, S., Pelletier, J. G., Ran, I., and Lacaille, J. C. (2009) *J. Neurosci.* **29,** 4658–4663
6. Neher, E. (1998) *Neuron* **20,** 389–399
7. Thalhammer, A., Rudhard, Y., Tigaret, C. M., Volynski, K. E., Rusakov, D. A., and Schoepfer, R. (2006) *EMBO J.* **25,** 5873–5883
8. Lee, S. J., Escobedo-Lozoya, Y., Szatmari, E. M., and Yasuda, R. (2009) *Nature* **458,** 299–304
9. De Koninck, P., and Schulman, H. (1998) *Science* **279,** 227–230
10. Morris, E. P., and Török, K. (2001) *J. Mol. Biol.* **308,** 1–8
11. Miller, S. G., Patton, B. L., and Kennedy, M. B. (1988) *Neuron* **1,** 593–604
12. Ohmae, S., Takemoto-Kimura, S., Okamura, M., Adachi-Morishima, A., Nonaka, M., Fuse, T., Kida, S., Tanji, M., Furuyashiki, T., Arakawa, Y., Narumiya, S., Okuno, H., and Bito, H. (2006) *J. Biol. Chem.* **281,** 20427–20439
13. Kemp, B. E., Pearson, R. B., House, C., Robinson, P. J., and Means, A. R. (1989) *Cell. Signal.* **1,** 303–311
14. Tzortzopoulos, A., Best, S. L., Kalamida, D., and Török, K. (2004) *Biochemistry* **43,** 6270–6280
15. Jama, A. M., Fenton, J., Robertson, S. D., and Török, K. (2009) *J. Biol. Chem.* **284,** 28146–28155
16. Martin, S. R., Andersson Teleman, A., Bayley, P. M., Drakenberg, T., and Forsen, S. (1985) *Eur. J. Biochem.* **151,** 543–550
17. Ikura, M., and Ames, J. B. (2006) *Proc. Natl. Acad. Sci. U.S.A.* **103,** 1159–1164
18. Xia, X. M., Fakler, B., Rivard, A., Wayman, G., Johnson-Pais, T., Keen, J. E., Ishii, T., Hirschberg, B., Bond, C. T., Lutsenko, S., Maylie, J., and Adelman, J. P. (1998) *Nature* **395,** 503–507
19. Török, K., Tzortzopoulos, A., Grabarek, Z., Best, S. L., and Thorogate, R. (2001) *Biochemistry* **40,** 14878–14890
20. Forest, A., Swulius, M. T., Tse, J. K., Bradshaw, J. M., Gaertner, T., and Waxham, M. N. (2008) *Biochemistry* **47,** 10587–10599
21. Evans, T. I., and Shea, M. A. (2009) *Proteins* **76,** 47–61
22. Tzortzopoulos, A., and Török, K. (2004) *Biochemistry* **43,** 6404–6414
23. Hashimoto, Y., and Soderling, T. R. (1987) *Arch. Biochem. Biophys.* **252,** 418–425
24. Török, K., Cowley, D. J., Brandmeier, B. D., Howell, S., Aitken, A., and Trentham, D. R. (1998) *Biochemistry* **37,** 6188–6198
25. Smith, G. L., and Miller, D. J. (1985) *Biochim. Biophys. Acta* **839,** 287–299
26. Linse, S., Helmersson, A., and Forsén, S. (1991) *J. Biol. Chem.* **266,** 8050–8054
27. Martin, S. R., Bayley, P. M., Brown, S. E., Porumb, T., Zhang, M., and Ikura, M. (1996) *Biochemistry* **35,** 3508–3517
28. Martin, S. R., Maune, J. F., Beckingham, K., and Bayley, P. M. (1992) *Eur. J. Biochem.* **205,** 1107–1114
29. Bradshaw, J. M., Hudmon, A., and Schulman, H. (2002) *J. Biol. Chem.* **277,** 20991–20998
30. Dodd, R., Peracchia, C., Stolady, D., and Török, K. (2008) *J. Biol. Chem.* **283,** 26911–26920
31. King, M. M., Shell, D. J., and Kwiatkowski, A. P. (1988) *Arch. Biochem. Biophys.* **267,** 467–473
32. Deleted in proof
33. Tadross, M. R., Dick, I. E., and Yue, D. T. (2008) *Cell* **133,** 1228–1240
34. Otmakhov, N., Tao-Cheng, J. H., Carpenter, S., Asrican, B., Dosemeci, A., Reese, T. S., and Lisman, J. (2004) *J. Neurosci.* **24,** 9324–9331
35. Shen, K., Teruel, M. N., Connor, J. H., Shenolikar, S., and Meyer, T. (2000) *Nat. Neurosci.* **3,** 881–886
36. Strack, S., and Colbran, R. J. (1998) *J. Biol. Chem.* **273,** 20689–20692
37. Migues, P. V., Lehmann, I. T., Fluechter, L., Cammarota, M., Gurd, J. W., Sim, A. T., Dickson, P. W., and Rostas, J. A. (2006) *J. Neurochem.* **98,** 289–299
38. Rose, J., Jin, S. X., and Craig, A. M. (2009) *Neuron* **61,** 351–358
39. Grant, P. A., Best, S. L., Sanmugalingam, N., Alessio, R., Jama, A. M., and Török, K. (2008) *Cell Calcium* **44,** 465–478
40. Shifman, J. M., Choi, M. H., Mihalas, S., Mayo, S. L., and Kennedy, M. B. (2006) *Proc. Natl. Acad. Sci. U.S.A.* **103,** 13968–13973